Histol Histopathol (2024) 39: 1167-1177

Histology and Histopathology
From Cell Biology to Tissue Engineering

ORIGINAL ARTICLE Open Access

Rapamycin mitigates organ damage by autophagy-mediated NLRP3 inflammasome inactivation in sepsis

Xiaofeng Li[1], Qingqiu Zeng[1], Rui Yao[2], Lingyan Zhang[1], Ying Kong[3] and Bin Shen[1]

[1]Department of Infectious Diseases, [2]Department of Intensive Care Units, Huzhou Central Hospital, Huzhou and [3]Department of Intensive Care Units, Changxing Traditional Chinese Medicine (TCM) Hospital, Changxing, PR China

Summary. Autophagy activation can alleviate sepsis-induced organ injuries. Rapamycin (Rap) has emerged as an autophagy regulator in multiple forms of organ injuries. This study aimed to assess whether Rap protects rats from cecal ligation and puncture (CLP)-induced sepsis through autophagy-mediated inactivation of the NLRP3 inflammasome. Rats were allocated to the sham, CLP, Rap (10 mg/kg), or 3-Methyladenine (3-MA) (15 mg/kg) groups. A rat CLP model was established. The survival of rats and lung wet-to-dry weight ratio in each group was assessed. Blood biochemical indexes and oxidative stress-related factors were analyzed with an automatic biochemical analyzer. The bacterial counts of blood and organs were monitored. The degrees of myeloperoxidase of the ileum, inflammation-related indexes, and pathological changes in the tissues were detected by ELISA and hematoxylin-eosin staining. The levels of NLRP3 inflammasome and autophagy-related factors were analyzed by Western blot. Rap increased the survival and SOD activity, and repressed ALT, AST, BUN, SCr, MDA, and inflammation-related marker levels in CLP rats, it also restrained the bacterial counts of blood, lung, liver, and kidney in CLP rats; the effects of 3-MA on CLP rats on the above-mentioned indicators were opposite to those of Rap. Additionally, Rap alleviated the pathological injury of the lung, liver, and kidney, which was the opposite to the effect of 3-MA on CLP rats. Furthermore, Rap mitigated the ASC, Pro-caspase 1, and NLRP3 levels and increased the Beclin-1 levels and the LC3II/LC3I ratio in the organ tissues. Collectively, autophagy activation can mitigate organ damage by suppressing the NLRP3 inflammasome in sepsis rats.

Key words: Sepsis, Autophagy, Rapamycin, 3-Methyladenine, NOD-like receptor family pyrin domain containing 3

Corresponding Author: Bin Shen, Department of Infectious Diseases, Huzhou Central Hospital, Huzhou, PR China. e-mail: shenbin_vip@126.com

www.hh.um.es. DOI: 10.14670/HH-18-706

Introduction

Sepsis is a life-threatening organ dysfunction resulting from the body's dysregulated response to infection, which is characterized by rapid onset, high clinical mortality, high cost, and continuous increase (Font et al., 2020). The major difference between sepsis and ordinary infection is that the body has abnormal or dysregulated reactions and organ dysfunction, which is a common acute and critical disease in intensive care units and one of the main causes of death in critically ill patients (Arvaniti et al., 2022). According to global statistics, more than 40 million patients suffer from sepsis in 2017, and mortality rates related to ICU-treated sepsis is as high as 41.9% (Fleischmann-Struzek et al., 2020; Rudd et al., 2020). The use of antibiotics and fluids in sepsis in its early stages can ameliorate the prognosis, but when these treatments fail, the mortality from septic shock still exceeds 40% (Levy et al., 2015; Seymour et al., 2017). Therefore, it is critical to identify potential adjuvant treatments for patients with sepsis.

It was proven that an increase in inflammatory factors, free radicals, and mitochondrial damage in sepsis, all lead to an increase in autophagy, which exhibits a significant modulatory role in sepsis (Han et al., 2021). The beneficial effect of autophagy activation in sepsis has been demonstrated in many animal models and cell experiments (Chung et al., 2017; Kimura et al., 2017; Sun et al., 2018). Autophagy is intimately related to inflammation and immunity, as well as the NLRP3 inflammasome (Qiu et al., 2019). Autophagy restrains the body's inflammatory response and alleviates tissue inflammatory damage by impeding the activation of the NLRP3 inflammasome (Cao et al., 2019). It is well known that proinflammatory cytokines, such as TNF-α, IL-1β, and IL-6, contribute to organ damage in patients with sepsis; inhibition of proinflammatory cytokines attenuates sepsis-related organ damage and ameliorates survival outcomes (Fatani et al., 2018; Al-Harbi et al., 2019; Zhao et al., 2019). Therefore, how to avoid damage to target organs caused by a "cytokine storm" is the current research hotspot.

Rapamycin (Rap) is a macrolide compound and a specific negative regulator of mammalian target of Rap (mTOR) signaling, which can impede mTOR signaling and facilitate autophagy (Takeuchi et al., 2005). A study suggested that the utilization of Rap to promote the activation of autophagy during sepsis could lessen the damage to cardiomyocytes and hepatocytes caused by sepsis, and notably ameliorate the survival rate of animal models of sepsis (Hsieh et al., 2011). 3-Methyladenine (3-MA), an autophagy inhibitor, lessened the Wnt pathway in diabetic retinas (Ye et al., 2021). The effect of 3-MA on multiple organ damage in sepsis remains unclear. Moreover, there are few studies on autophagy preventing multiple organ damage and inflammatory response in sepsis by regulating the NLRP3 inflammasome, and further studies are needed to prove the inhibition effect of autophagy on the NLPR3 inflammasome in the pathophysiology of sepsis.

In this study, cecal ligation and puncture (CLP) was applied to establish a rat model of sepsis. The effects of Rap on multiple organizations of CLP rats were discussed regarding liver and kidney function damage, the histopathology of lung, liver, and kidney, NLRP3 inflammasome, and autophagy-related protein changes. This study offers a scientific basis for the investigation of sepsis pathogenesis and offers a novel idea for the treatment of sepsis.

Materials and methods

Ethics statement

All animal manipulations were reviewed and ratified by the Institutional Animal Care and Use Committee. All animal experiments were performed following protocols approved by the Ethics Committee of Zhejiang Eyong Pharmaceutical Research and Development Center (SYXK (Zhe) 2021-0033).

Animals

Male Sprague-Dawley (SD) rats (n=44), weighing 220-230 g, were procured from Shanghai Jihui Laboratory Animal Care Co., Ltd. with the certificate number SCXK (Hu) 2017-0012. All animals were acclimatized for seven days under the standard conditions (20±2°C, humidity 60±10%, and light/dark cycle for 12h).

Establishment of a rat CLP model

All rats were randomized into the sham group, CLP group, CLP+Rapamycin (Rap, V900930, Sigma-Aldrich, USA) group, and CLP+3-Methyladenine (3-MA, M9281, Sigma-Aldrich, USA) group, with 14 rats in each group. CLP surgery was carried out as follows (Chen et al., 2019): deep anesthesia was performed with isoflurane (induced at 4% and maintained at 3%). We made a 2 cm incision in the abdominal midline of SD rats and then ligated the midpoint between the cecum valve and the cecum with a sterile 4-0 surgical suture. After that, we used a no. 21 needle to puncture the ligated cecum twice. Finally, the laparotomy incision was sutured layer by layer. SD rats in the sham group underwent the same procedures except ligation and puncture. All rats were resuscitated with normal saline after surgery.

Drug treatment

One hour after CLP, SD rats in the CLP+Rap group and 3-MA group were intraperitoneally injected with Rap at 10 mg/kg and 3-MA at 15 mg/kg for one day, respectively (Han et al., 2018; Jia et al., 2019). SD rats in the sham group and CLP group were injected with equal volumes of saline intraperitoneally, one hour after the operation.

Survival analysis

After CLP, the survival rate of eight rats in each group on the first, second, third, fifth, and seventh day after the operation was monitored and counted.

Sample collection

Twenty-four hours after the experiment, three SD rats in each group were anesthetized with 3% isoflurane. Blood samples were gathered from the right ventricle of SD rats by cardiac puncture. The harvested blood samples underwent centrifugation (3500 r/min, 15 min). At the end of the blood collection, the anesthetized SD rats underwent perfusion with 150 mL of normal saline through the heart and incised the right atrial appendage. Thereafter, SD rats were subjected to perfusion with 300 mL 4% paraformaldehyde (PFA, M002, GEFAN, China) until the tissues hardened. Afterward, the lung, liver, and kidney tissues were removed and fixed in 4% PFA overnight. Then, the tissues were dehydrated and embedded in paraffin. The paraffin blocks were cut into 5-μm sections.

Detection of blood biochemical indexes

In this study, the contents of alanine amino-transferase (ALT), aspartate aminotransferase (AST), blood urea nitrogen (BUN), serum creatinine (Scr), malondialdehyde (MDA), and superoxide dismutase (SOD) levels in the serum of each group were assessed with utilizing an automatic biochemical analyzer (C16000, Abbott, USA).

Wet/dry weight ratio of lung

The removed lung tissues were rinsed with phosphate buffer solution and then blotted with absorbent paper. Next, the lung tissues were weighted, i.

e., wet weight. Thereafter, the lung tissues were placed in a 70°C oven to a constant weight. Then, the lung wet-to-dry weight ratio was calculated.

ELISA

The quantification of tissue cytokines was evaluated by applying ELISA. The rat myeloperoxidase (MPO) ELISA kit (MM-0337R1) was acquired from MEIMIAN (China). Frozen rat ileum tissue samples underwent homogenization. The concentration of MPO was assessed in the whole-tissue extracts via ELISA following the operation instructions and displayed as U/g of total proteins. For measurement of serum IL-1β, IL-4, TNF-α, and IFN-γ in each group, the IL-1β assay kit (MM-0040M1), IL-4 assay kit (MM-0191R1), TNF-α assay kit (MM-0132M1), and IFN-γ assay kit (MM-0198R1) were used. Serum levels of inflammatory markers were detected according to the operating instructions of these kits.

Bacterial counts

Blood, lung, liver, and kidney were collected and homogenized in 2 mL of sterile PBS 24h post-administration. The homogenized blood and organs were serially diluted and then spread on LB agar plates. After incubation at 37°C for one day, colonies were counted and displayed as colony-forming counts (CFU)/organ.

Hematoxylin and eosin (H&E) staining

For the assessment of pathological changes in lung, liver, and kidney tissues, an H&E staining kit (G1003, Servicebio, China) was selected. After being dewaxed with xylene, the tissue sections underwent rehydration in gradient alcohols (100%, 95%, 85%, and 70%), and were then stained with hematoxylin for 5 min. After being differentiated with 1% hydrochloric acid for 30 s, the sections were reacted with 1% eosin solution for 120 s. After dehydration, sections were subjected to coverslip in neutral balsam (36313ES60, Yeasen, China). In the end, changes in organ sections were observed with the assistance of an optical microscope (Eclipse E100, Nikon, Japan). The lung, liver, and kidney injuries were graded based on a scoring system in a blinded fashion from 0 (normal) to 4 (severe) as described previously (Smith et al., 1997; Coimbra et al., 2005; Yasuda et al., 2006).

Western blot

For the lysis of organ tissues, RIPA buffer (P0013D) supplied by Beyotime (China) was applied. Next, a BCA kit (pc0020, Solarbio, China) was chosen to quantify the total protein concentration. After denaturation and electrophoresis, the separated protein was transferred onto a PVDF membrane, which was then sealed with 5% bovine serum albumin (BSA, 4240GR100, BioFRoxx, Germany) at 37°C for 1h. After that, the sealed membrane was incubated with primary antibodies (4°C, overnight) and then Anti-Rabbit IgG H&L (HRP) antibody (1:5000, ab7090, Abcam, UK) at 37°C for 1h. After visualization with ECL reagent (36208ES60, YEASEN, China), a gel imaging system (610020-9Q, Clinx, China) was selected to expose the protein bands. The primary antibodies of ASC (1:10000, ab151700) and Pro-caspase 1 (1:1000, ab179515) were bought from Abcam (UK). The primary antibodies of Beclin-1 (1:2000, AF5128), LC3A/B (1:2000, AF5402), NLRP3 (1:1000, DF7438), and GAPDH (1:10000, AF7021) were from Affinity (USA).

Statistics

Data from these experiments were reported as mean ± standard deviation. For statistical analysis, SPSS software (16.0, IBM, USA) was utilized. One-way ANOVA with the Tukey test was employed for multiple comparisons. Kruskal-Wallis H test was applied for the measurement of data that do not conform to normal distributions. A *P-value* <0.05 was considered significant. In addition, Kaplan Meier curves showed survival rates and underwent log-rank analysis; Bonferroni correction was applied to correct *P-values* for multiple testing of Kaplan Meier curves (Bonferroni corrected *P-value* <0.05/6≈0.0083).

Results

The effects of Rap and 3-MA on the survival, oxidative stress, and systemic inflammatory response of CLP rats

The survival analysis of rats revealed that CLP caused a significant decrease in survival in rats (Fig. 1A) (P<0.0083). Relative to the CLP group, the survival of rats in the CLP+Rap group was higher and the survival of rats in the CLP+3-MA group was lower (Fig. 1A); survival rates on day 7 were 12.5%, 62.5%, and 0%, respectively. There was no significant statistical difference between the CLP + Rap and CLP + 3-MA groups compared with the CLP group, however, their trend does suggest that Rap intervention may be effective in improving survival rates in sepsis. By detecting blood biochemical indexes, we found that the concentrations of ALT, AST, BUN, and SCr, examined with an automatic biochemical analyzer, were notably increased in CLP rats (Fig. 1B-E, P<0.01). CLP-induced up-regulation of ALT, AST, BUN, and SCr concentrations was repressed by Rap (Fig. 1B-E, P<0.05). Furthermore, 3-MA largely enhanced the levels of ALT, AST, BUN, and SCr in CLP rats (Fig. 1B-E, P<0.01). In Figure 1F, compared with sham rats, CLP obviously augmented the lung wet-to-dry weight ratio of rats, which was reversed by Rap (Fig. 1F, P<0.05). The increase in the lung wet-to-dry weight ratio is closely related to acute lung injury induced by sepsis (Li et al., 2022). CLP prominently facilitated MPO in the rat ileum, whereas Rap partially offset its effect (Fig. 1G, P<0.01). 3-MA effectively increased MPO in the ileum

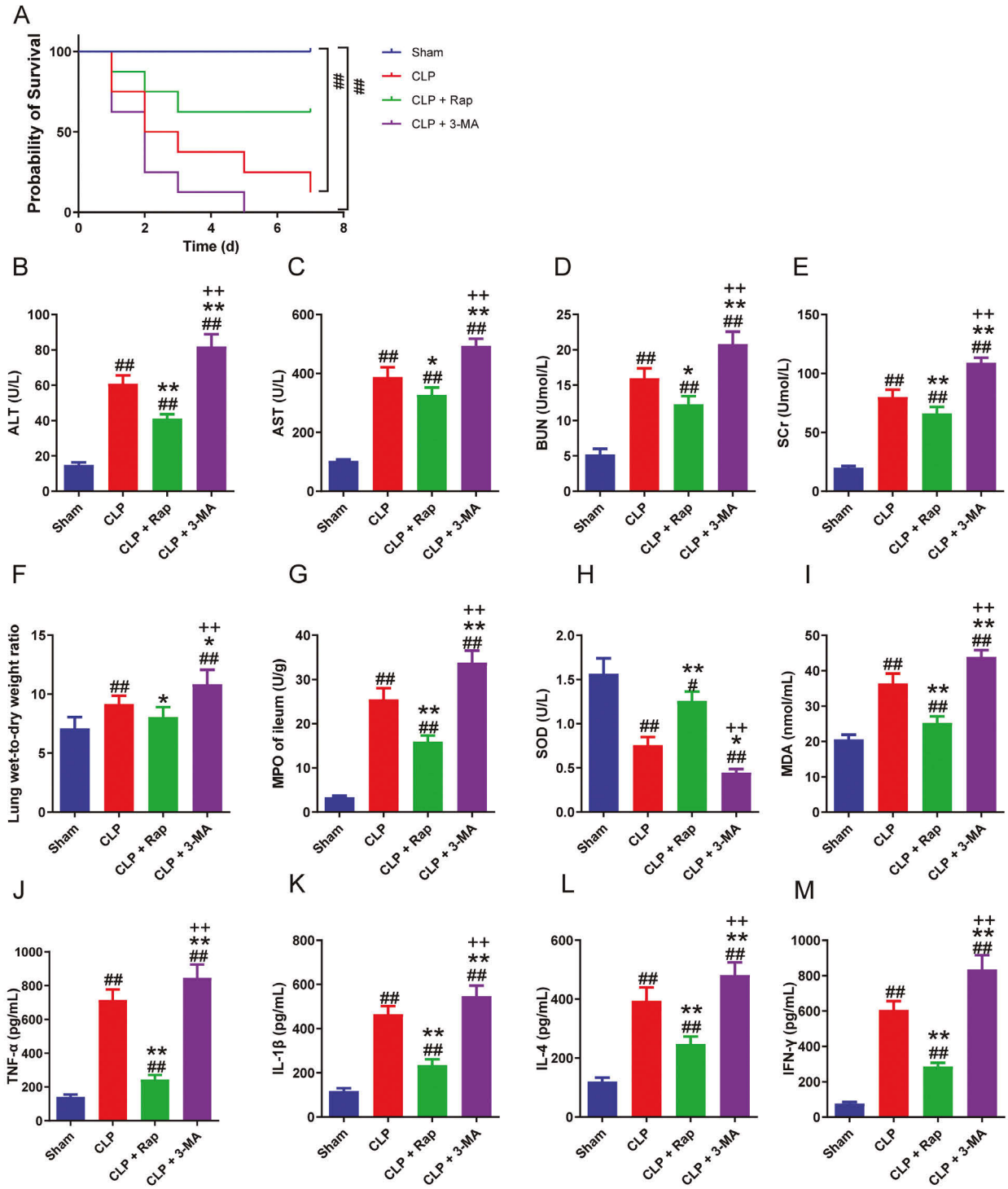

Fig. 1. The effects of Rap and 3-MA on the survival, oxidative stress, and systemic inflammatory response of CLP rats. **A.** Rap improved the survival rate of CLP rats, while 3-MA decreased it (n=8). Kaplan Meier curves showing the survival rates were analyzed using log-rank analysis; Bonferroni correction was applied to correct P-values for multiple testing (Bonferroni corrected *P*-value<0.05/6≈0.0083). **B-E.** Serum biochemistries of CLP rats were reduced by Rap treatment, and 3-MA upregulated them (n=6). **F.** The wet-to-dry weight ratio of the lung in CLP rats was reduced by Rap and increased by 3-MA (n=6). **G.** Rap treatment decreased MPO in the ileum of CLP rats while 3-MA treatment raised it (n=6). **H, I.** Related indicators of oxidative stress indexes, SOD and MDA, were improved by Rap treatment, while 3-MA aggravated them (n=6). **J-M.** The levels of TNF-α, IL-1β, IL-4, and INF-γ were reduced by Rap and increased by 3-MA treatment (n=6). Data are presented as the mean ± standard deviation. $^{\#\#}P$<0.01 vs. the sham group; $^{*}P$<0.05, $^{**}P$<0.01 vs. the CLP group; ^{++}P<0.01 vs. the CLP + Rap group. Abbreviations: CLP: cecal ligation and puncture; Rap: Rapamycin; 3-MA: 3-methyladenine; MPO: myeloperoxidase; SOD: superoxide dismutase; MDA: malondialdehyde; TNF-α: tumor necrosis factor-α; IL: interleukin.

of CLP rats compared with the CLP group (Fig. 1G, $P<0.01$). Then, we examined oxidative stress- and inflammation-related markers. In CLP group, decreased serum SOD levels and augmented serum MDA, TNF-α, IL-1β, IL-4, and IFN-γ levels in rats were observed (Fig. 1H-M, $P<0.01$); these aforementioned relevant markers induced by CLP were reversed by Rap (Fig. 1H-M, $P<0.01$). The intervention of 3-MA led to lower serum SOD concentrations and higher serum MDA, TNF-α, IL-1β, IL-4, and IFN-γ levels in CLP rats (Fig. 1H-M, $P<0.01$).

The effects of Rap and 3-MA on the bacterial burden of CLP rats

As seen in Figure 2A-D, Rap was discovered to restrain the bacterial counts of blood, lung, liver, and kidney in CLP rats ($P<0.01$), while 3-MA strongly enhanced them (Fig. 2A-D, $P<0.01$).

The effects of Rap and 3-MA on the histological injury, NLRP3 inflammasome, and autophagy-related markers in the lung of CLP rats

H&E staining results showed that there were no pathological changes in the lung tissues of rats in the sham group; in the CLP group, relative to the sham group, the alveolar number and wall thickness were increased, additionally, a small amount of inflammatory cell accumulation was present. Compared with the CLP group, the alveolar cavity in the CLP + Rap group was more intact with a small amount of inflammatory cell aggregation, and the number of alveoli was decreased; while in the CLP + 3-MA group, the alveolar cavity was narrowed and alveolar wall thickness increased accompanied by obviously inflammatory cell aggregation (Fig. 3A). The results of H&E semi-quantitative scoring results revealed that lung tissues of the CLP group scored evidently higher than that those of the sham group; while the CLP + Rap group scored lower, and the CLP + 3-MA group scored notably higher than the CLP group (Fig. 3B, $P<0.05$). The results of Western blot analysis showed that there were increments in ASC, Pro-caspase 1, Beclin-1, and NLRP3 protein levels, and the ratio of LC3II/LC3I in the CLP group compared with the sham group (Fig. 3C-H, $P<0.01$). Rap intervention prominently diminished the expressions of ASC, Pro-caspase 1, and NLRP3 and increased the ratio of LC3II/LC3I in the lung tissues of CLP rats (Fig. 3C-H, $P<0.05$). Furthermore, 3-MA treatment effectively augmented ASC, Pro-caspase 1, and NLRP3 levels and suppressed Beclin-1 levels and the ratio of LC3II/LC3I in the lung tissues of CLP rats (Fig. 3C-H, $P<0.05$).

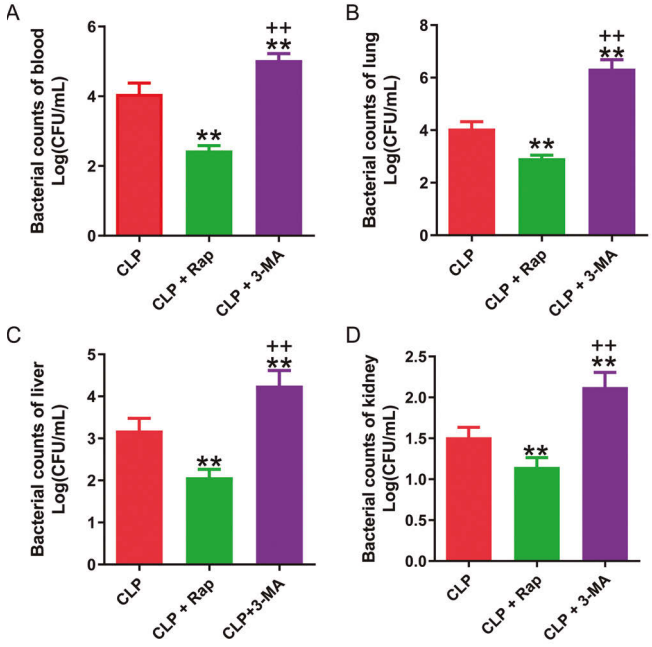

Fig. 2. The effects of Rap and 3-MA on the bacterial burden of CLP rats. The bacterial burden of blood **(A)**, lungs **(B)**, liver **(C)**, and kidneys **(D)** were reduced by Rap treatment, while 3-MA treatment increased them. Data are presented as the mean ± standard deviation. $^{**}P<0.01$ vs. the CLP group; $^{++}P<0.01$ vs. the CLP + Rap group. Abbreviation: CLP: cecal ligation and puncture; 3-MA: 3-methyladenine.

The effects of Rap and 3-MA on the histological injury, NLRP3 inflammasome, and autophagy-related markers in the liver of CLP rats

There was no significant pathological damage in liver tissues of the rats in the sham group; there was a small amount of inflammatory cell infiltration in liver tissues of CLP group rats, and hepatocytes were closely arranged, while Rap treatment attenuated this histological damage; 3-MA further advanced the infiltration of inflammatory cells into the liver tissues of CLP rats and the arrangement of hepatocytes was loose (Fig. 4A). The facilitation of CLP induction of the H&E semi-quantitative score of liver tissues was reversed by Rap, while 3-MA further strengthened the promotion of CLP on the H&E semi-quantitative score of liver tissues (Fig. 4B, $P<0.05$). We also examined the expression of the NLRP3 inflammasome and autophagy-related proteins in liver tissues of CLP rats, found that Rap evidently alleviated the levels of ASC, Pro-caspase 1, and NLRP3 and augmented the ratio of LC3II/LC3I in liver tissues of CLP rats, whereas the modulation of 3-MA on the ASC, pro-caspase 1, NLRP3, and Beclin-1 expression and the ratio of LC3II/LC3I in the liver tissues of CLP rats was contrary to that of Rap (Fig. 4C-H, $P<0.05$).

The effects of Rap and 3-MA on the histological injury, NLRP3 inflammasome, and autophagy-related markers in the kidney of CLP rats

In Figure 5A, rat renal tissues in the CLP group exhibited some inflammatory cell infiltration,

accompanied by a small amount of epithelial cell swelling and shedding, which was further aggravated by 3-MA (Fig. 5A). Compared with the CLP group, in the CLP + Rap group, the alveolar cavity was intact and there was a small amount of inflammatory cell infiltration, but there was no swelling or shedding of epithelial cells (Fig. 5A). The modulatory effects of Rap and 3-MA on the H&E semi-quantitative score of renal tissues in CLP rats were coincident with that of liver and lung tissues (Fig. 5B, $P<0.05$). In addition, Western blot results showed that 3-MA further heightened the upregulation of CLP induction on the levels of ASC,

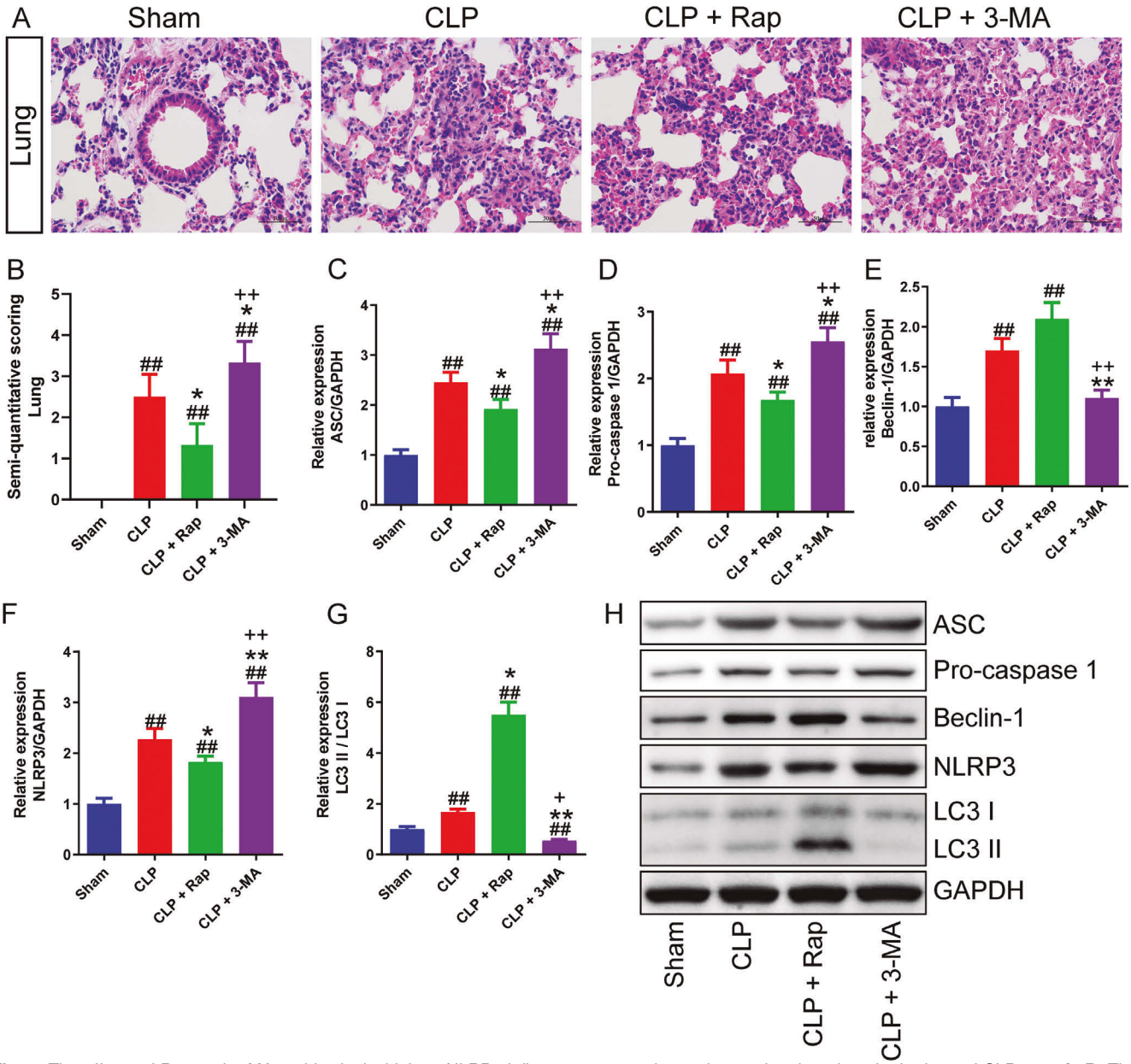

Fig. 3. The effects of Rap and 3-MA on histological injury, NLRP3 inflammasome, and autophagy-related markers in the lung of CLP rats. **A, B.** The degree of lung tissue damage was observed by H&E staining (n=6). According to the integrity of the lung tissues and the degree of inflammatory cell aggregation, the degree of lung damage was scored, being proportional to the score. **C-H.** The NLRP3 inflammasome and autophagy-related protein levels of the lung were measured by Western blot (n=3). The levels of ASC, pro-caspase 1, and NLRP3 protein in the lungs of CLP rats were reduced by Rap treatment, and the Beclin-1 and ratio of LC3II to I levels were increased by Rap treatment, while 3-MA treatment had the contrary effect. Data are presented as the mean ± standard deviation. $^{\#\#}P<0.01$ vs. the sham group; $^{*}P<0.05$, $^{**}P<0.01$ vs. the CLP group; $^{++}P<0.01$ vs. the CLP + Rap group. Abbreviations: CLP: cecal ligation and puncture; 3-MA: 3-methyladenine; H&E staining: hematoxylin-eosin staining; ASC: apoptosis-associated speck-like protein containing a CARD; NLRP3: NOD-like receptor thermal protein domain associated protein 3; LC3: microtubule-associated proteins light chain 3, MAP1LC3.

Pro-caspase 1, and NLRP3 and counteracted the promotion of CLP induction on Beclin-1 levels and the ratio of LC3II/LC3I in kidney tissues (Fig. 5C-H, $P<0.05$). The introduction of Rap prominently inhibited ASC, Pro-caspase 1, and NLRP3 levels and advanced the Beclin-1 levels and the ratio of LC3II/LC3I in the kidney tissues (Fig. 5C-H, $P<0.05$).

Discussion

At present, sepsis is one of the most challenging health problems in the world, with increasing morbidity and mortality, and no effective treatment (Tang et al., 2017; Hunt, 2019). In this study, the CLP method was exploited to establish a rat model of diffuse peritonitis

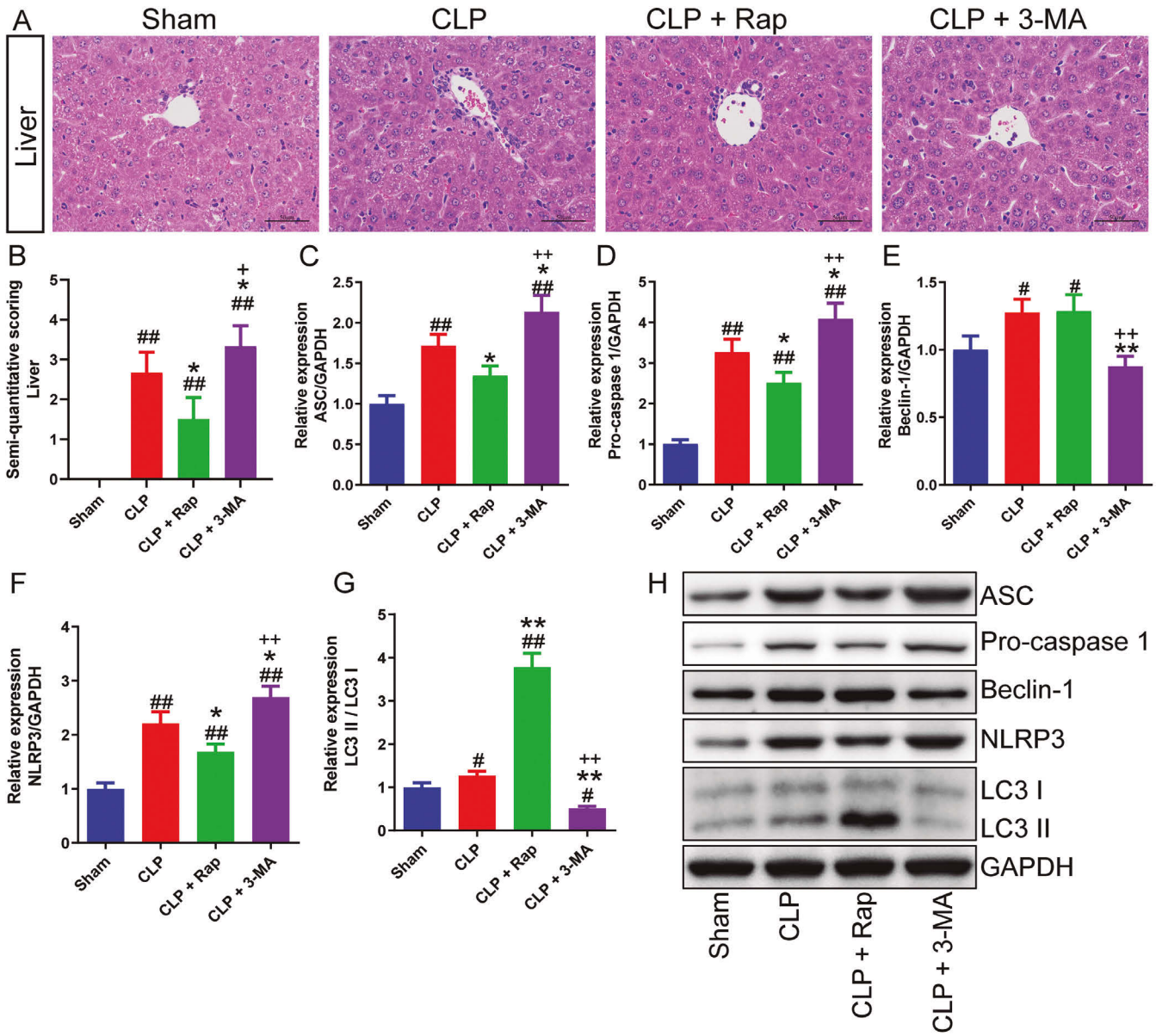

Fig. 4. The effects of Rap and 3-MA on the histological injury, NLRP3 inflammasome, and autophagy-related markers in the liver of CLP rats. **A, B.** The degree of liver tissue damage was observed by H&E staining (n=6). According to the degree of inflammatory cell infiltration and loose arrangement of hepatocytes, the degree of liver damage was scored, the degree being proportional to the score. **C-H.** The NLRP3 inflammasome and autophagy-related protein levels of the liver were measured by Western blot (n=3). The levels of ASC, pro-caspase 1, and NLRP3 protein in the livers of CLP rats were reduced by Rapamycin, and the ratio of LC3 II to I levels was increased, while 3-MA treatment had the contrary effect. Also, the Beclin-1 levels were reduced by 3-MA treatment. Data are presented as the mean ± standard deviation. $^{\#}P<0.05$, $^{\#\#}P<0.01$ vs. the sham group; $^{*}P<0.05$, $^{**}P<0.01$ vs. the CLP group; $^{+}P<0.05$, $^{++}P<0.01$ vs. the CLP + Rap group. Abbreviations: CLP: cecal ligation and puncture; 3-MA: 3-methyladenine; H&E staining: hematoxylin-eosin staining; ASC: apoptosis-associated speck-like protein containing a CARD; NLRP3: NOD-like receptor thermal protein domain associated protein 3; LC3: microtubule-associated proteins light chain 3, MAP1LC3.

and simulate a disease course similar to clinical sepsis (Drechsler and Osuchowski, 2021). Sepsis can lead to multiple organs failure throughout the body, including the kidney, liver, and lungs (Zhi et al., 2019). This study checked the impacts of the autophagy activator Rap and autophagy inhibitor 3-MA on sepsis-related organ failure by assessing kidney function-related indicators (BUN and Scr) and liver enzymes (ALT and AST). Scr and BUN are specific indicators for measuring clinical renal function (Zaki et al., 2018). AST and ALT are

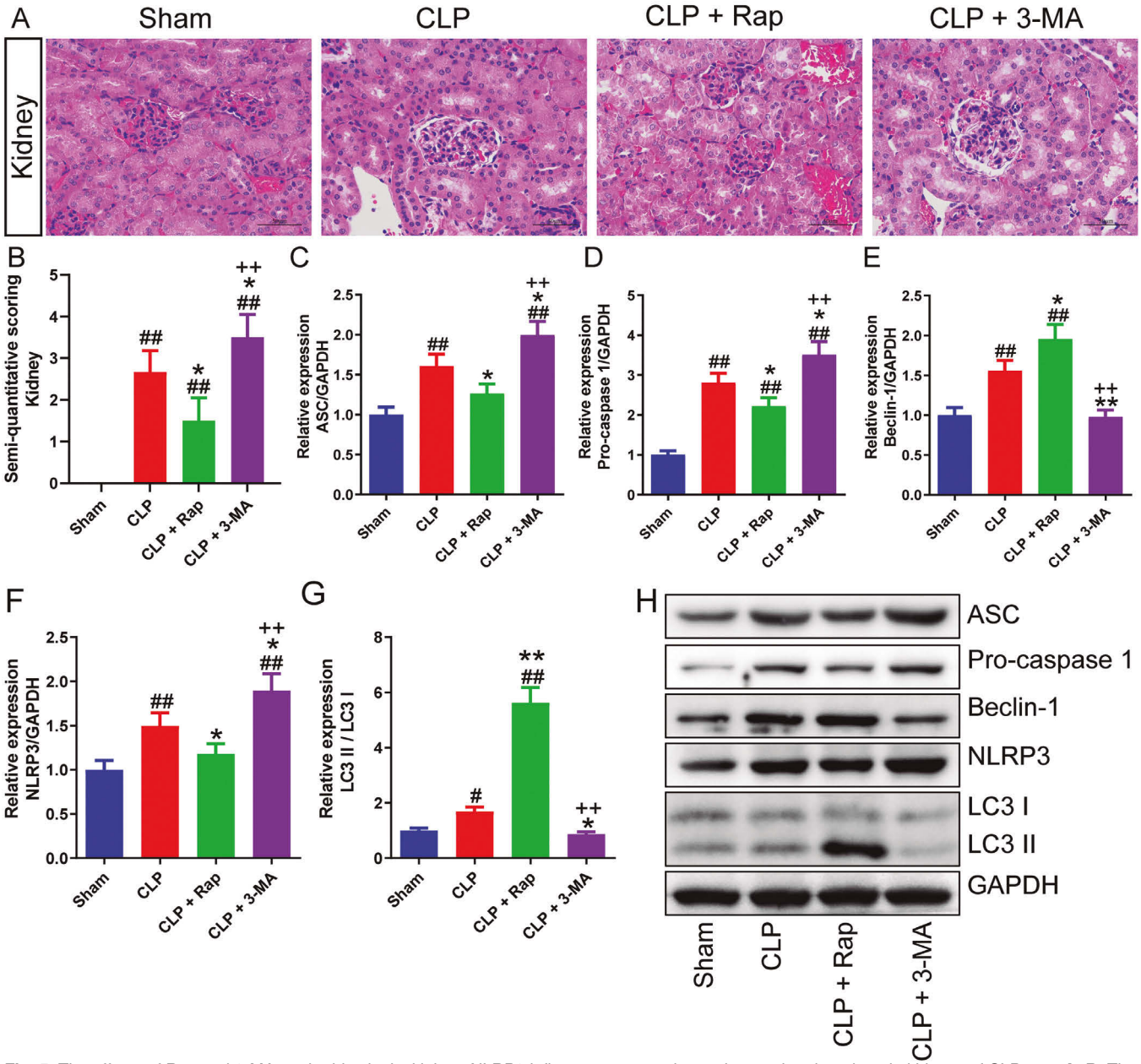

Fig. 5. The effects of Rap and 3-MA on the histological injury, NLRP3 inflammasome, and autophagy-related markers in kidneys of CLP rats. **A, B.** The degree of kidney tissue damage was observed by H&E staining (n=6). According to the degree of inflammatory cell infiltration and the swelling and shedding of epithelial cells, the degree of kidney damage was scored, the degree being proportional to the score. **C-H.** The NLRP3 inflammasome and autophagy-related protein levels of the kidneys were measured by Western blot (n=3). The levels of ASC, pro-caspase 1, and NLRP3 protein in the lungs of CLP rats were reduced by Rapamycin treatment, and Beclin-1 and the ratio of LC3 II to I levels were increased by Rapamycin treatment, while 3-MA treatment had the contrary effect. Data are presented as the mean ± standard deviation. $^{\#\#}P<0.01$ vs. the sham group; $^{*}P<0.05$, $^{**}P<0.01$ vs. the CLP group; $^{+}P<0.05$, $^{++}P<0.01$ vs. the CLP + Rap group. Abbreviations: CLP: cecal ligation and puncture; 3-MA: 3-methyladenine; H&E staining: hematoxylin-eosin staining; ASC: apoptosis-associated speck-like protein containing a CARD; NLRP3: NOD-like receptor thermal protein domain associated protein 3; LC3: microtubule-associated proteins light chain 3, MAP1LC3.

transaminases in the liver and kidney, which are released intracellularly when tissues are damaged (Hung et al., 2017). This study found that CLP-induced upregulation of ALT, AST, BUN, and SCr concentrations was repressed by Rap, whereas 3-MA largely enhanced these levels of ALT, AST, BUN, and SCr in CLP rats, suggesting that autophagy activation could ameliorate liver and kidney function in septic rats.

It was reported that sepsis was tightly related to oxidative stress (Xu et al., 2021). The concentration of MDA dose not only reflect the degree of oxidative stress damage, but it is also an indicate for indirect measurement of cell injury (Wei et al., 2014). Rap has been extensively demonstrated to have protective effects against various diseases such as Parkinson's disease, diabetes, and heterotopic ossification by restraining oxidative stress (Xiang et al., 2020; Hu and Wang, 2021). Li et al. clarified that autophagy could repress oxidative stress (Li et al., 2017). By conducting ELISA analysis, Rap was discovered to increase SOD levels and restrain MDA levels in CLP rat serum, illustrating that the autophagy inducer impeded the oxidative stress response in CLP rats. Furthermore, Rap displayed antifungal activity for *Candida albicans* (Tong et al., 2021). Autophagy functions as a defense mechanism against invading intracellular pathogens, targeting both vacuolar and cytosolic pathogens (Chong et al., 2012). Some scholars showed that activation of autophagy could lessen the intracellular bacterial load (Wang et al., 2021). In this study, the bacterial counts in the blood, liver, kidney, and lung were notably higher in the CLP group than in the Rap + CLP group, suggesting that Rap manifested intense bactericidal capacity in CLP rats.

As a result of diverse organ inflammation caused by sepsis, body organs are damaged. Scientists observed that the heart, lungs, liver, and kidneys suffered various degrees of functional damage in sepsis (Khosrojerdi et al., 2021). In this study, the results from H&E staining discovered that Rap alleviated histological injuries of the liver, kidney, and lung tissues in CLP rats. Han's team reported that the rat model of sepsis was prepared by the CLP method, and the limitation of autophagy in cardiomyocytes could aggravate myocardial injury in sepsis; the use of the autophagy inducer Rap to upregulate the autophagy level of cardiomyocytes could mitigate the pathological myocardial damage and injury caused by CLP, ameliorate myocardial hypoxia, and alleviate the contractile dysfunction of cardiomyocytes caused by sepsis, suggesting that promoting the autophagy of cardiomyocytes can alleviate cardiac dysfunction (Han et al., 2018). Additionally, Lin et al. found that, by facilitating autophagy in liver cells, serum transaminase levels could be lower, the degree of liver damage in sepsis could be alleviated, and the survival rate of septic rats could be improved (Lin et al., 2014). A previous report clarified that damaged mitochondria in sepsis were associated with the NLRP3 inflammasome (Danielski et al., 2020). Autophagy could negatively modulate the activation of the NLRP3 inflammasome, thereby impeding the body's inflammatory response (Chang et al., 2015; Biasizzo and Kopitar-Jerala, 2020).

The NLRP3 inflammasome can activate ASC and caspase-1, thereby causing the maturation and release of the pro-inflammatory factor IL-1β, resulting in the expansion of the inflammatory response (Sharma and Kanneganti, 2016). Moreover, the NLRP3 inflammasome can be stimulated and activated by a variety of pathogenic microorganisms and danger signals and is involved in the initiation and progression of a variety of diseases, including severe systemic infection (sepsis), multiple sclerosis, and type 2 diabetes (Lamkanfi and Dixit, 2014; Lu et al., 2020). NLRP3 is intimately related to multi-organ damage in sepsis, and inhibition of NLRP3 inflammasome activation in septic rats can suppress the release of caspase-1 and IL-1β, thereby stabilizing vascular endothelial cadherin and alleviating sepsis-induced lung injury (Zhong et al., 2020). Scientific studies indicated that autophagy induced by Rap exerted a protective effect on a variety of diseases, such as chronic nonbacterial prostatitis, autoimmune diseases, and cardiac injury, by inhibiting inflammation mediated by the NLRP3 inflammasome (Ko et al., 2017; Lu et al., 2019; Yu et al., 2020). This study confirmed that Rap mitigated the ASC, Pro-caspase 1, and NLRP3 levels and promoted the Beclin-1 levels and the LC3II/LC3I ratio of liver, lung, and kidney tissues in CLP rats, revealing that Rap protected rats from CLP-induced sepsis by mitigating the autophagy-NLRP3 axis-mediated inflammatory response. This study observed the protective effect of intraperitoneal injection of Rap after CLP on the lung, liver, and kidney tissues of septic rats. It is necessary to further analyze the effects of different doses and administration times on the organ tissues in sepsis.

Interestingly, a study reported that 3-MA intervention in mice before CLP modeling can improve the survival rate of CLP mice (Li et al., 2018). However, another stud demonstrated that drug interventions promoting autophagy after CLP can enhance organ protection in septic rats, but 3-MA can act as an antagonist (Jia et al., 2019). Results of this study showed that administering 3-MA post-CLP injury promotes inflammation and exacerbates organ damage in rats. These findings underscore the importance of carefully considering drug intervention timing when treating sepsis and warrant further investigation.

Taken together, all data confirmed that the activation of autophagy protected against organ injuries induced by sepsis, and its mechanism may be correlated with the autophagy-NLRP3 axis-mediated inflammatory response. Thus, the activation of autophagy to regulate the NLRP3 inflammasome can protect against multiple organ injury in septic rats.

Acknowledgements. N/A.

Conflict of Interests. There are no competing interests between authors.

Funding. This study was supported by the Zhejiang Medical and Health Science and Technology Project (LGF22H190006)

Data availability. Data will be made available upon request.

References

Al-Harbi N.O., Nadeem A., Ahmad S.F., Alanazi M.M., Aldossari A.A. and Alasmari F. (2019). Amelioration of sepsis-induced acute kidney injury through inhibition of inflammatory cytokines and oxidative stress in dendritic cells and neutrophils respectively in mice: Role of spleen tyrosine kinase signaling. Biochimie 158, 102-110.

Arvaniti K., Dimopoulos G., Antonelli M., Blot K., Creagh-Brown B., Deschepper M., De Lange D., De Waele J., Dikmen Y., Eckmann C., Einav S., Francois G., Fjeldsoee-Nielsen H., Girardis M., Jovanovic B., Lindner M., Koulenti D., Labeau S., Lipman J., Lipovestky F., Makikado L.D.U., Maseda E., Mikstacki A., Montravers P., Paiva J.A., Pereyra C., Rello J., Timsit J.F., Tomescu D., Vogelaers D., Blot S. and Abdominal Sepsis Study (AbSeS) Group on behalf of the Trials Group of the European Society of Intensive Care Medicine (2022). Epidemiology and age-related mortality in critically ill patients with intra-abdominal infection or sepsis: an international cohort study. Int. J. Antimicrob. Agents 60, 106591.

Biasizzo M. and Kopitar-Jerala N. (2020). Interplay between NLRP3 inflammasome and autophagy. Front. Immunol. 11, 591803.

Cao Z., Wang Y., Long Z. and He G. (2019). Interaction between autophagy and the NLRP3 inflammasome. Acta Biochim. Biophys. Sin. (Shanghai) 51, 1087-1095.

Chang Y.P., Ka S.M., Hsu W.H., Chen A., Chao L.K., Lin C.C., Hsieh C.C., Chen M.C., Chiu H.W., Ho C.L., Chiu Y.C., Liu M.L. and Hua K.F. (2015). Resveratrol inhibits NLRP3 inflammasome activation by preserving mitochondrial integrity and augmenting autophagy. J. Cell Physiol. 230, 1567-1579.

Chen J.X., Xu X. and Zhang S. (2019). Silence of long noncoding RNA NEAT1 exerts suppressive effects on immunity during sepsis by promoting microRNA-125-dependent MCEMP1 downregulation. IUBMB Life 71, 956-968.

Chong A., Wehrly T.D., Child R., Hansen B., Hwang S., Virgin H.W. and Celli J. (2012). Cytosolic clearance of replication-deficient mutants reveals Francisella tularensis interactions with the autophagic pathway. Autophagy 8, 1342-1356.

Chung K.W., Kim K.M., Choi Y.J., An H.J., Lee B., Kim D.H., Lee E.K., Im E., Lee J., Im D.S., Yu B.P. and Chung H.Y. (2017). The critical role played by endotoxin-induced liver autophagy in the maintenance of lipid metabolism during sepsis. Autophagy 13, 1113-1129.

Coimbra R., Porcides R.D., Melbostad H., Loomis W., Tobar M., Hoyt D.B. and Wolf P. (2005). Nonspecific phosphodiesterase inhibition attenuates liver injury in acute endotoxemia. Surg. Infect. (Larchmt), 6, 73-85.

Danielski L.G., Giustina A.D., Bonfante S., Barichello T. and Petronilho F. (2020). The NLRP3 inflammasome and its role in sepsis development. Inflammation 43, 24-31.

Drechsler S. and Osuchowski M. (2021). Cecal ligation and puncture. Methods Mol. Biol. 2321, 1-8.

Fatani S.H., Aa A.L., Al-Amodi H.S., Kamel H.F., Al-Khatieb K. and Bader H. (2018). Assessment of tumor necrosis factor alpha polymorphism TNF-α_{-238} (rs 361525) as a risk factor for development of acute kidney injury in critically ill patients. Mol. Biol. Rep. 45, 839-847.

Fleischmann-Struzek C., Mellhammar L., Rose N., Cassini A., Rudd K.E., Schlattmann P., Allegranzi B. and Reinhart K. (2020). Incidence and mortality of hospital- and ICU-treated sepsis: results from an updated and expanded systematic review and meta-analysis. Intensive Care Med. 46, 1552-1562.

Font M.D., Thyagarajan B. and Khanna A.K. (2020). Sepsis and septic shock - Basics of diagnosis, pathophysiology and clinical decision making. Med. Clin. North Am. 104, 573-585.

Han W., Wang H., Su L., Long Y., Cui N. and Liu D. (2018). Inhibition of the mTOR pathway exerts cardioprotective effects partly through autophagy in CLP rats. Mediators Inflamm. 2018, 4798209.

Han D., Fang R., Shi R., Jin Y. and Wang Q. (2021). LncRNA NKILA knockdown promotes cell viability and represses cell apoptosis, autophagy and inflammation in lipopolysaccharide-induced sepsis model by regulating miR-140-5p/CLDN2 axis. Biochem. Biophys. Res. Commun. 559, 8-14.

Hsieh C.H., Pai P.Y., Hsueh H.W., Yuan S.S. and Hsieh Y.C. (2011). Complete induction of autophagy is essential for cardioprotection in sepsis. Ann. Surg. 253, 1190-1200.

Hu Y. and Wang Z. (2021). Rapamycin prevents heterotopic ossification by inhibiting the mTOR pathway and oxidative stress. Biochem. Biophys. Res. Commun. 573, 171-178.

Hung Y.L., Fang S.H., Wang S.C., Cheng W.C., Liu P.L., Su C.C., Chen C.S., Huang M.Y., Hua K.F., Shen K.H., Wang Y.T., Suzuki K. and Li C.Y. (2017). Corylin protects LPS-induced sepsis and attenuates LPS-induced inflammatory response. Sci. Rep. 7, 46299.

Hunt A. (2019). Sepsis: an overview of the signs, symptoms, diagnosis, treatment and pathophysiology. Emerg. Nurse 27, 32-41.

Jia J., Gong X., Zhao Y., Yang Z., Ji K., Luan T., Zang B. and Li G. (2019). Autophagy enhancing contributes to the organ protective effect of alpha-lipoic acid in septic rats. Front. Immunol. 10, 1491.

Khosrojerdi A., Soudi S., Hosseini A.Z., Eshghi F., Shafiee A. and Hashemi S.M. (2021). Immunomodulatory and therapeutic effects of mesenchymal stem cells on organ dysfunction in sepsis. Shock (Augusta, Ga.) 55, 423-440.

Kimura T., Isaka Y. and Yoshimori T. (2017). Autophagy and kidney inflammation. Autophagy 13, 997-1003.

Ko J.H., Yoon S.O., Lee H.J. and Oh J.Y. (2017). Rapamycin regulates macrophage activation by inhibiting NLRP3 inflammasome-p38 MAPK-NFκB pathways in autophagy- and p62-dependent manners. Oncotarget 8, 40817-40831.

Lamkanfi M. and Dixit V.M. (2014). Mechanisms and functions of inflammasomes. Cell 157, 1013-1022.

Levy M.M., Rhodes A., Phillips G.S., Townsend S.R., Schorr C.A., Beale R., Osborn T., Lemeshow S., Chiche J.D., Artigas A. and Dellinger R.P. (2015). Surviving sepsis campaign: association between performance metrics and outcomes in a 7.5-year study. Crit. Care Med. 43, 3-12.

Li D.Y., Yu J.C., Xiao L., Miao W., Ji K., Wang S.C. and Geng Y.X. (2017). Autophagy attenuates the oxidative stress-induced apoptosis of Mc3T3-E1 osteoblasts. Eur. Rev. Med. Pharmacol. Sci. 21, 5548-5556.

Li Q., Li L., Fei X., Zhang Y., Qi C., Hua S., Gong F. and Fang M. (2018). Inhibition of autophagy with 3-methyladenine is protective in a lethal model of murine endotoxemia and polymicrobial sepsis. Innate Immun. 24, 231-239.

Li Z.F., Wang Y.C., Feng Q.R., Zhang Y.S., Zhuang Y.F., Xie Z.X. and Bai X.J. (2022). Inhibition of the C3a receptor attenuates sepsis-induced acute lung injury by suppressing pyroptosis of the pulmonary vascular endothelial cells. Free Radic. Biol. Med. 184, 208-217.

Lin C.W., Lo S., Perng D.S., Wu D.B., Lee P.H., Chang Y.F., Kuo P.L.,

Yu M.L., Yuan S.S. and Hsieh Y.C. (2014). Complete activation of autophagic process attenuates liver injury and improves survival in septic mice. Shock (Augusta, Ga.) 41, 241-249.

Lu J., Su Y., Chen X., Chen Y., Luo P., Lin F. and Zhang J. (2019). Rapamycin-induced autophagy attenuates hormone-imbalance-induced chronic non-bacterial prostatitis in rats via the inhibition of NLRP3 inflammasome-mediated inflammation. Mol. Med. Rep. 19, 221-230.

Lu F., Lan Z., Xin Z., He C., Guo Z., Xia X. and Hu T. (2020). Emerging insights into molecular mechanisms underlying pyroptosis and functions of inflammasomes in diseases. J. Cell. Physiol. 235, 3207-3221.

Qiu P., Liu Y. and Zhang J. (2019). Review: the role and mechanisms of macrophage autophagy in sepsis. Inflammation 42, 6-19.

Rudd K.E., Johnson S.C., Agesa K.M., Shackelford K.A., Tsoi D., Kievlan D.R., Colombara D.V., Ikuta K.S., Kissoon N., Finfer S., Fleischmann-Struzek C., Machado F.R., Reinhart K.K., Rowan K., Seymour C.W., Watson R.S., West T.E., Marinho F., Hay S.I., Lozano R., Lopez A.D., Angus D.C., Murray C.J.L. and Naghavi M. (2020). Global, regional, and national sepsis incidence and mortality, 1990-2017: analysis for the global burden of disease study. Lancet 395, 200-211.

Seymour C.W., Gesten F., Prescott H.C., Friedrich M.E., Iwashyna T.J., Phillips G.S., Lemeshow S., Osborn T., Terry K.M. and Levy M.M. (2017). Time to treatment and mortality during mandated emergency care for sepsis. N. Engl. J. Med. 376, 2235-2244.

Sharma D. and Kanneganti T.D. (2016). The cell biology of inflammasomes: Mechanisms of inflammasome activation and regulation. J. Cell Biol. 213, 617-629.

Smith K.M., Mrozek J.D., Simonton S.C., Bing D.R., Meyers P.A., Connett J.E. and Mammel M.C. (1997). Prolonged partial liquid ventilation using conventional and high-frequency ventilatory techniques: gas exchange and lung pathology in an animal model of respiratory distress syndrome. Crit. Care Med. 25, 1888-1897.

Sun Y., Yao X., Zhang Q.J., Zhu M., Liu Z.P., Ci B., Xie Y., Carlson D., Rothermel B.A., Sun Y., Levine B., Hill J.A., Wolf S.E., Minei J.P. and Zang Q.S. (2018). Beclin-1-dependent autophagy protects the heart during sepsis. Circulation 138, 2247-2262.

Takeuchi H., Kondo Y., Fujiwara K., Kanzawa T., Aoki H., Mills G.B. and Kondo S. (2005). Synergistic augmentation of rapamycin-induced autophagy in malignant glioma cells by phosphatidylinositol 3-kinase/protein kinase B inhibitors. Cancer Res. 65, 3336-3346.

Tang H., Liang Y.B., Chen Z.B., Du L.L., Zeng L.J., Wu J.G., Yang W., Liang H.P. and Ma Z.F. (2017). Soluble egg antigen activates M2 macrophages via the STAT6 and PI3K pathways, and schistosoma japonicum alternatively activates macrophage polarization to improve the survival rate of septic mice. J. Cell Biochem. 118, 4230-4239.

Tong Y., Zhang J., Wang L., Wang Q., Huang H., Chen X., Zhang Q., Li H., Sun N., Liu G., Zhang B., Song F., Alterovitz G., Dai H. and Zhang L. (2021). Hyper-Synergistic antifungal activity of rapamycin and peptide-like compounds against Candida albicans orthogonally via Tor1 kinase. ACS Infect. Dis. 7, 2826-2835.

Wang Z., Lan R., Xu Y., Zuo J., Han X., Phouthapane V., Luo Z. and Miao J. (2021). Taurine alleviates streptococcus uberis-induced inflammation by activating autophagy in mammary epithelial cells. Front. Immunol. 12, 631113.

Wei B., Li W.W., Ji J., Hu Q.H. and Ji H. (2014). The cardioprotective effect of sodium tanshinone IIA sulfonate and the optimizing of therapeutic time window in myocardial ischemia/reperfusion injury in rats. Atherosclerosis 235, 318-327.

Xiang H., Zhang J., Lin C., Zhang L., Liu B. and Ouyang L. (2020). Targeting autophagy-related protein kinases for potential therapeutic purpose. Acta Pharm. Sin. B 10, 569-581.

Xu S., Li L., Wu J., An S., Fang H., Han Y., Huang Q., Chen Z. and Zeng Z. (2021). Melatonin attenuates sepsis-induced small-intestine injury by upregulating SIRT3-mediated oxidative-stress inhibition, mitochondrial protection, and autophagy induction. Front. Immunol. 12, 625627.

Yasuda H., Yuen P.S., Hu X., Zhou H. and Star R.A. (2006). Simvastatin improves sepsis-induced mortality and acute kidney injury via renal vascular effects. Kidney Int. 69, 1535-1542.

Ye S., Zhang Y., Wang X., Liang X., Wei M., Zong R., Liu Z. and Chen Q. (2021). Autophagy positively regulates Wnt signaling in mice with diabetic retinopathy. Exp. Ther. Med. 22, 1164.

Yu W., Qin X., Zhang Y., Qiu P., Wang L., Zha W. and Ren J. (2020). Curcumin suppresses doxorubicin-induced cardiomyocyte pyroptosis via a PI3K/Akt/mTOR-dependent manner. Cardiovasc. Diagn. Ther. 10, 752-769.

Zaki O.S., Safar M.M., Ain-Shoka A.A. and Rashed L.A. (2018). Bone marrow mesenchymal stem cells combat lipopolysaccharide-induced sepsis in rats via amendment of P38-MAPK signaling cascade. Inflammation 41, 541-554.

Zhao Y., Nie M., Xu P., Li H., Xu L., Cheng X.Q. and Lei Y.Q. (2019). Nitrosporeusine A attenuates sepsis-associated acute kidney injury through the downregulation of IL-6/sIL-6R axis activation-mediated PGC-1α suppression. Biochem. Biophys. Res. Commun. 515, 474-480.

Zhi D.Y., Lin J., Zhuang H.Z., Dong L., Ji X.J., Guo D.C., Yang X.W., Liu S., Yue Z., Yu S.J. and Duan M.L. (2019). Acute kidney injury in critically III patients with sepsis: Clinical characteristics and outcomes. J. Invest. Surg. 32, 689-696.

Zhong M., Wu W., Wang Y., Mao H., Song J., Chen S. and Zhu D. (2020). Inhibition of sphingosine kinase 1 attenuates sepsis-induced microvascular leakage via inhibiting macrophage NLRP3 inflammasome activation in mice. Anesthesiology 132, 1503-1515.

Accepted January 9, 2024